Measurement of the Elliptical Birefringence of Single-Mode Optical Fibers

Article *in* Applied Optics · November 2001

DOI: 10.1364/AO.40.005343 · Source: PubMed

Measurement of the elliptical birefringence of single-mode optical fibers

Thierry Chartier, Ammar Hideur, Cafer Özkul, François Sanchez, and Guy M. Stéphan

The polarization properties of single-mode optical fibers are theoretically modeled with use of the Jones formalism. The fiber is described as an elliptical birefringent plate. The properties predicted by this model are discussed and lead to the development of a simple experimental method to extract the parameters that describe a real fiber. A magneto-optic method that measures the beat length of the fiber is also presented and gives a more complete description of the fiber. The validity of the model is then clearly established. Finally, the wavelength dependence of the parameters characteristic of the fiber is experimentally investigated. © 2001 Optical Society of America

OCIS codes: 060.2400, 260.1440, 260.5430, 140.3510.

1. Introduction

Polarization properties of single-mode optical fibers are the subject of many studies. The main concern of scientists since the early days of research[1,2] has been the modeling of the complicated nature of birefringence exhibited by fibers. This unexpected property of fibers is due to imperfections and causes two polarizations to propagate at different group velocities. In the field of optical communications, where light propagates over kilometers, the birefringence induces polarization-mode dispersion and limits the performance of high-bit-rate communication systems.[3,4] A useful tool in characterizing this limiting phenomenon is the use of the principal states of polarization.[3–5] In the field of rare-earth doped-fiber amplifiers and lasers, where the fiber length is, at maximum, some tens of meters, it is often more convenient to take into account the birefringence of the fiber through a simple Jones matrix formalism.[6–9] In this paper, we examined the polarization properties of optical fibers in the latter context.

Even if polarization-dependent losses are neglected, the modeling of the fiber remains complicated, essentially because of the complicated nature of birefringence. Indeed, it is generally admitted that the fiber exhibits locally (i.e., for a thin section of fiber) linear birefringence induced by small geometric anisotropy of the core, residual stress, or local bending.[1,2] The fiber thus can be locally characterized by the simple Jones matrix of a linear retarder. Because a real fiber is not necessarily homogeneous or undergoes twists[10] or winding,[11] it has to be considered as a succession of wave plates possessing arbitrary birefringence and orientation. This view has led researchers to consider random fluctuation of birefringence[12,13] or random mode coupling[14,15] in the fiber. In this case, the equivalent Jones matrix of the fiber is not supposed to give a local description of the polarization properties of the fiber but must be seen as a global transfer function, linking the Jones vector of an output state of polarization to the corresponding input Jones vector. In the most general case this Jones matrix is the one of an elliptical birefringent plate, i.e., a wave plate whose polarization eigenstates are elliptical.

The purpose of this paper is to present a simple formalism for the Jones matrix of the fiber, to investigate the properties of such a model, and to present experimental methods to determine exactly the parameters of the model. Section 2 is devoted to the presentation of the model. We first present the Jones matrix of the fiber in a general formulation requiring three parameters and the choice of an ar-

T. Chartier (Thierry.chartier@coria.fr), A. Hideur, and C. Özkul are with the Groupe d'Optique et d'Optronique, Complexe de Recherche Interprofessionnel en Aérothermochimie, Unité Mixte de Recherche 6614, Université de Rouen, Place Emile Blondel, 76821 Mont-Saint-Aignan cedex, France. F. Sanchez is with the Laboratoire des Propriétés Optiques des Matériaux et Applications, Université d'Angers, 2 Bd. Lavoisier, 49045 Angers cedex 01, France. G. M. Stephan is with the Laboratoire d'Optronique, École Nationale Supérieure de Sciences Appliquées et de Technologie, 6 rue de Kérampont, 22305 Lannion cedex, France.

Received 17 November 2000; revised manuscript received 18 May 2001.

0003-6935/01/305343-11$15.00/0

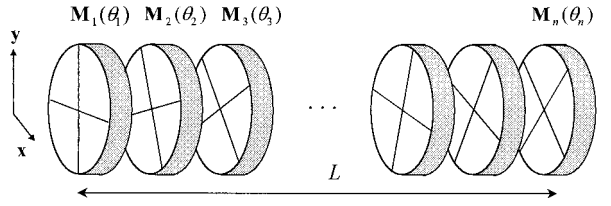

Fig. 1. Description of the fiber as a concatenation of birefringent plates $\mathbf{M}_i$ oriented along θ_i.

bitrary basis. We show that the choice of a more practical basis allows us to obtain a reduced model requiring only two parameters that have physical meaning. In Section 3 we investigate the properties of this model. We point out some particular states of polarization that permit us to develop a simple experimental method to find the parameters of the model for a given fiber. In Section 4, we present the experimental method that simply consists of measuring the azimuth of three linear polarizations. A magneto-optic (MO) method is also used to measure the beat length of the fiber considered to be an elliptical retarder. The wavelength dependence of the parameters is also investigated. In this situation we show that, depending on the wavelength of the injected signal, the same fiber can act like an elliptical, a circular, or a linear birefringent plate.

2. Model for the Fiber

As mentioned in the introduction, the fiber can be seen as the concatenation of a large number of thin linear birefringent plates,[13] with some plates oriented differently from others, as described in Fig. 1. If we neglect any polarization-dependent losses, the Jones matrix $\mathbf{M}_f$ of the fiber, in an arbitrary basis ($\mathbf{x}$, $\mathbf{y}$), is then the product of a large number of matrices of linear retarders and rotation matrices[16]:

$$\mathbf{M}_f = \mathbf{R}(\theta_n)\mathbf{M}_n\mathbf{R}(-\theta_n)\ldots \times \mathbf{R}(\theta_2)\mathbf{M}_2\mathbf{R}(-\theta_2)\mathbf{R}(\theta_1)\mathbf{M}_1\mathbf{R}(-\theta_1), \quad (1)$$

where $\mathbf{R}(\theta)$ is the rotation matrix of angle θ given by

$$\mathbf{R}(\theta) = \begin{pmatrix} \cos\theta & -\sin\theta \\ \sin\theta & \cos\theta \end{pmatrix}. \quad (2)$$

Let us note that $\mathbf{R}(\theta)$ is also the matrix of a medium that would have purely circular birefringence like optical activity or the Faraday effect. $\mathbf{M}_i$ is the matrix of a linear birefringent:

$$\mathbf{M}_i = \begin{pmatrix} \exp\left(i\,\frac{\varphi_i}{2}\right) & 0 \\ 0 & \exp\left(-i\,\frac{\varphi_i}{2}\right) \end{pmatrix}, \quad (3)$$

where φ_i is the phase difference. For long fibers submitted to any kind of internal or external perturbations, the longitudinal description of the fiber fails, and θ and φ_i can be considered to be random. On the other hand, one can know exactly the longitudinal

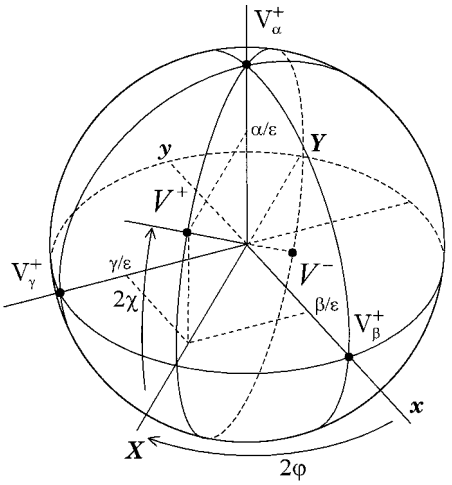

Fig. 2. Eigenvectors $\mathbf{V}^{\pm}$ of $\mathbf{M}_f$ on the Poincaré sphere.

dependence of θ and φ_i. This is, for example, the case for short-length polarization-maintaining fibers submitted to a homogeneous twist. In all cases the description of the fiber by use of Eq. (1) is true, and the formalism of $\mathbf{M}_f$ remains the same.

This kind of calculus, considering a medium with both linear and circular birefringence, was first performed by Jones.[17] Its associated Jones matrix is the one of an elliptical birefringent. In the most general case, for a fiber of length L in an arbitrary basis ($\mathbf{x}$, $\mathbf{y}$), it is expressed as[12,17,18]:

$$\mathbf{M}_f = \begin{pmatrix} a & b \\ -b^* & a^* \end{pmatrix}, \quad (4)$$

with

$$a = \cos\frac{\epsilon L}{2} + i\,\frac{\beta}{\epsilon}\sin\frac{\epsilon L}{2}, \quad (5)$$

$$b = -\frac{\alpha + i\gamma}{\epsilon}\sin\frac{\epsilon L}{2}, \quad (6)$$

$$\epsilon = (\alpha^2 + \beta^2 + \gamma^2)^{1/2}. \quad (7)$$

We see that, for a complete description of the matrix, this model requires three real parameters: α, β, and γ. All these parameters are expressed in radians/meter. The parameter ϵ represents the total phase difference per unit length and will be referred to in the following as the elliptical birefringence of the fiber. The quantity ϵL is then the total phase difference between the two polarization eigenstates. In the case of an elliptical birefringent, these eigenstates are two orthogonal elliptical polarizations. They can thus be described by their ellipticity χ and azimuth φ for one polarization and $-\chi$ and $\varphi + \pi/2$ for the other. Both 2χ and 2φ are angles representing one eigenstate of polarization on the Poincaré sphere as represented in Fig. 2. According to Jones,[17] α is related to the circular part of the elliptical birefringence, β is related to the linear part whose eigenaxes are parallel to the $\mathbf{x}$ and $\mathbf{y}$ axes, and

γ is related to the linear part whose eigenaxes are parallel to the bisectors of **x** and **y**. If only one of the parameters α, β, γ is different from zero (for example, $\alpha \neq 0$, $\beta = 0$, and $\gamma = 0$), the eigenstates of the corresponding matrix are $\mathbf{V}_\alpha^\pm$, $\mathbf{V}_\beta^\pm$, or $\mathbf{V}_\gamma^\pm$, depending on which of the three parameters is different from zero ($\mathbf{V}_\alpha^\pm$ in the previous example). According to Fig. 2, the three eigenstates $\mathbf{V}_\alpha^\pm$, $\mathbf{V}_\beta^\pm$, and $\mathbf{V}_\gamma^\pm$ (and, equivalently, the three parameters α, β, and γ) define a basis on which any elliptical birefringent can be decomposed.

The link between the three parameters α, β, γ and the two angles χ, φ can be deduced from the previous geometrical considerations (see Fig. 2) or can be found by calculation of eigenvectors $\mathbf{V}^\pm$ of $\mathbf{M}_f$ and by use of Appendix A. In both cases, we find

$$\sin 2\chi = \frac{\alpha}{\epsilon}, \tag{8}$$

$$\tan 2\varphi = -\frac{\gamma}{\beta}. \tag{9}$$

Note that ϵ is given as a function of α, β, γ by Eq. (7). At this stage, the fiber is then characterized by either (α, β, γ) or (ϵ, χ, φ).

The basis (**x**, **y**) in which $\mathbf{M}_f$ is written is arbitrary. Any change in its orientation would affect the value of α, β, and γ. However, there is no restriction in choosing a basis for which the value of γ is zero, leading to, according to Fig. 2 or Eq. (9), $\varphi = 0$. In this case, the problem of the experimental determination of matrix $\mathbf{M}_f$ of the fiber would then reduce to find only two parameters (α and β) and the basis in which the matrix is written.

Thus in the new basis (**X**, **Y**), rotated by φ with respect to the former reference of $\mathbf{M}_f$ (see Fig. 2), the Jones matrix $\mathbf{M}_f'$ of the fiber is expressed as

$$\mathbf{M}_f' = \begin{pmatrix} a' & b' \\ -b' & a'* \end{pmatrix}, \tag{10}$$

where parameters a' and b' are then given by

$$a' = \cos\frac{\epsilon L}{2} + i\,\frac{\beta'}{\epsilon}\sin\frac{\epsilon L}{2}, \tag{11}$$

$$b' = -\frac{\alpha}{\epsilon}\sin\frac{\epsilon L}{2}, \tag{12}$$

with

$$\epsilon = (\alpha^2 + \beta'^2)^{1/2}. \tag{13}$$

Note that α and ϵ are not affected by the change of the basis. The difference with the previous model lies in the fact that b' is now real, since $\gamma' = 0$. In the following, the model for the fiber will be given by Eqs. (10)–(13), where the primes will be omitted for simplicity. At this stage, the Jones matrix of the fiber is then characterized by the two parameters α and β and the basis (**X**, **Y**). The parameter α is the circular part of the birefringence of the fiber, whereas β corresponds to the linear part.[8–10,19] The basis (**X**, **Y**) coincides with the azimuth of the eigenpolarizations of the fiber and, as will be seen in Section 3, offers a more practical property. Note that, according to Fig. 2, the ellipticity χ of $\mathbf{V}^+$ is still given by

$$\sin 2\chi = \frac{\alpha}{\epsilon}. \tag{14}$$

3. Polarization Properties of the Model

In this section we theoretically study the properties of the matrix of an elliptical birefringent given by Eqs. (10)–(13) to propose simple measurement methods of the parameters describing the matrix.

A. Linear States of Polarization

One of the fundamental properties of any elliptical birefringent, which have already been pointed out in optical fibers,[12,14] is the following: There always exist two orthogonal and linear input polarizations that also exit the fiber linearly polarized, but with a different azimuth. Let us call $\mathbf{L}_{in}$ one of these linear states of polarization (LSP) and $\mathbf{L}_{out}$ its corresponding output state. Since $\mathbf{L}_{in}$ is linear we set

$$\mathbf{L}_{in} = \begin{pmatrix} \cos\,\phi_{in} \\ \sin\,\phi_{in} \end{pmatrix}, \tag{15}$$

where ϕ_{in} is the azimuth of $\mathbf{L}_{in}$. To determine ϕ_{in} we first calculate $\mathbf{L}_{out}$ by using

$$\mathbf{L}_{out} = \mathbf{M}_f\mathbf{L}_{in}. \tag{16}$$

Then, by use of Appendix A, the third Stokes parameter s_3 of $\mathbf{L}_{out}$ is taken equal to zero, since the polarization state must be linear. This relation gives ϕ_{in}. Knowing ϕ_{in} we can then calculate the azimuth ϕ_{out} of $\mathbf{L}_{out}$ by using Eq. (16) and Appendix A. After some algebra we find the following results:

$$\phi_{out} = -\phi_{in} = \phi, \tag{17}$$

with

$$\tan 2\phi = \frac{\alpha}{\epsilon}\tan\frac{\epsilon L}{2}. \tag{18}$$

Equation (17) implies that ϕ_{out} is the symmetric of ϕ_{in} with respect to the **X** axis. The experimental determination of ϕ_{out} and ϕ_{in} allows us to find the orientation of the basis (**X**, **Y**) in which the model is written and then gives the azimuths of the polarization eigenstates of the fiber. To define matrix $\mathbf{M}_f$ of the fiber completely we have to find α and β. Knowledge of ϕ_{out} and ϕ_{in} provides more interesting information. Indeed, we can evaluate the quantity $2\phi = \phi_{out} - \phi_{in}$, which links parameters α and ϵ through Eq. (18). Let us note that in the following we prefer to determine ϵ instead of β. At this stage of our study, another equation is needed to find α and ϵ. This relation could be Eq. (14) and would then require us to measure the ellipticity of the eigenpolarizations of the fiber. As will be seen in Section 3.B, we prefer a

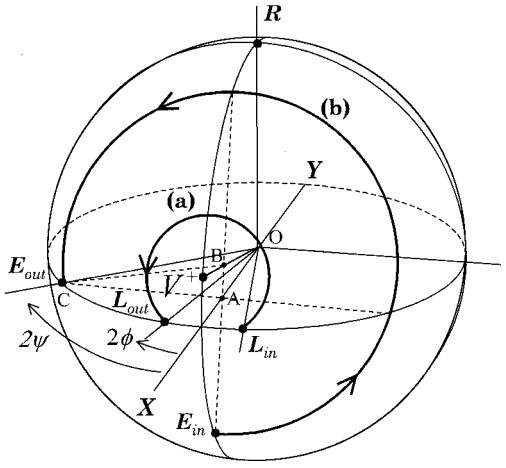

Fig. 3. Representation on the Poincaré sphere of the LSP and the ESP and the paths (a) and (b) representing their transformation by the fiber.

more accurate method that requires the measurement of the azimuth of a linear polarization.

The LSPs are represented in Fig. 3. In this figure **R** is the right-handed circular polarization represented by a positive ellipticity. For simulation of $\mathbf{M}_f$ on the Poincaré sphere, we used the following values: $L = 1$ m, $\alpha = 1$ rad/m, and $\beta = 4.8$ rad/m. These values are lower than those measured on a real fiber but permit us to illustrate our discussion. Path (a) represents the evolution of an input LSP, $\mathbf{L}_{\text{in}}$, that propagates in the fiber. Note that the modeling of the fiber as a single Jones matrix $\mathbf{M}_f$, resulting from the concatenation of a large number of wave plates, cannot realistically describe the longitudinal evolution of a polarization state injected in the fiber. However, according to Fig. 3, $\mathbf{M}_f$ appears to be a useful tool in simulating the transformation of input polarizations by the fiber. The input LSP, $\mathbf{L}_{\text{in}}$, is then transformed in $\mathbf{L}_{\text{out}}$ by the fiber, and Fig. 3 confirms that these two states of polarization are symmetric with respect to the **X** axis.

B. Elliptical States of Polarization

In this subsection we present the second procedure leading to a second equation to determine α and ϵ. This measurement is based on the following property we found for an elliptical birefringent: There always exist two orthogonal elliptical input polarizations, with the same azimuth as the eigenstates of the fiber, that exit the fiber linearly polarized. To calculate the input ellipticity and the output azimuth of these so-called elliptical states of polarization (ESP), we have to set

$$\mathbf{E}_{\text{out}} = \mathbf{M}_f \mathbf{E}_{\text{in}}, \tag{19}$$

where $\mathbf{E}_{\text{in}}$ is the input polarization with an ellipticity of ξ and an azimuth equal to zero and can thus be written as

$$\mathbf{E}_{\text{in}} = \begin{pmatrix} \cos \xi \\ i \sin \xi \end{pmatrix}. \tag{20}$$

To find the azimuth ψ of the output ESP $\mathbf{E}_{\text{out}}$ we set its Stokes parameter s_3 equal to zero (see Appendix A). After some algebra, we obtain

$$\tan 2\psi = \frac{\alpha}{\epsilon} \tan \epsilon L \tag{21}$$

for an input ellipticity of

$$\tan 2\xi = \frac{\alpha\beta(1 - \cos \epsilon L)}{\alpha^2 + \beta^2 \cos \epsilon L}. \tag{22}$$

The interesting formula is Eq. (21), because it gives another simple equation for α and ϵ. In Fig. 3 the path (b) of the injected state $\mathbf{E}_{\text{in}}$ that exits the fiber along $\mathbf{E}_{\text{out}}$ is also represented.

It is interesting to note that Fig. 3 also provides some geometric confirmations of the results obtained in this subsection. For example, it is obvious that in this figure

$$OA = \cos 2\psi, \tag{23}$$

$$AC = \sin 2\psi, \tag{24}$$

$$AB = OA \sin 2\chi = \frac{\alpha}{\epsilon} \cos 2\psi. \tag{25}$$

Then, the angle of rotation ϵL can be expressed as follows:

$$\tan \epsilon L = \frac{AC}{AB} = \frac{\epsilon}{\alpha} \tan 2\psi. \tag{26}$$

Equation (26) is similar to Eq. (21) obtained by use of the Jones matrix formalism. This geometric method can also be applied to find the expressions of 2φ and 2ξ.

C. Determination of the Parameters

The previous subsections, concerning the polarization properties of any fiber modeled as an elliptical birefringent, have led to an experimental method to determine the Jones matrix of the fiber. The method consists of finding the LSP and the ESP of the fiber and of measuring the azimuths of $\mathbf{L}_{\text{in}}$, $\mathbf{L}_{\text{out}}$, and $\mathbf{E}_{\text{out}}$. The angle medium of the first two azimuths ($\phi_{\text{in}} = -\phi$ and $\phi_{\text{out}} = \phi$) gives the azimuth of the polarization eigenstate of the fiber and then the orientation of the basis (**X**, **Y**) in which the matrix of the fiber is written with use of α and ϵ. The last two azimuths (ϕ and ψ) give two other equations [Eqs. (18) and (21)], containing α and ϵ. Note that the originality of the method lies in the fact that it consists of measuring only the azimuth of three linear polarizations that can be easily realized with a polarizer. Using Eqs. (18) and (21), we can introduce the quantity m defined by

$$\tan \frac{\epsilon L}{2} = \pm \left[1 - 2 \frac{\tan 2\phi}{\tan 2\psi} \right]^{1/2} = \pm m, \tag{27}$$

and then we find

$$\epsilon = \frac{2}{L}\,(\pm\arctan m \pm k\pi), \tag{28}$$

$$\alpha = \pm\frac{\epsilon}{m}\tan 2\phi, \tag{29}$$

$$\beta = \pm(\epsilon^2 - \alpha^2)^{1/2}, \tag{30}$$

where k is an integer ($k \geq 0$). We now examine the symmetry properties of the equations to simplify the previous relations. It is obvious from Eqs. (11) and (12) that the sign of ϵ does not affect matrix $\mathbf{M}_f$ of the fiber; in other words, $\mathbf{M}_f(-\epsilon) = \mathbf{M}_f(\epsilon)$. By convention we chose $\epsilon > 0$. It is easy to show that a change in the sign of β leads to a rotation of $\pi/2$ of the basis in which the matrix of the fiber is written, i.e., $\mathbf{M}_f(-\beta) = \mathbf{R}(\pi/2)\mathbf{M}_f(\beta)\mathbf{R}(-\pi/2)$. Since the basis ($\mathbf{X}$, $\mathbf{Y}$) is defined as modulo $\pi/2$, by convention we choose to call $\mathbf{X}$ the azimuth of the polarization eigenstate with a positive (right-handed) ellipticity, which means $\beta > 0$. The parameter α represents the rotation (per unit length) that is due to circular birefringence. The sign of α determines whether the rotation is clockwise (dextrorotatory) or counterclockwise (levorotatory).[20] With our convention, given by Eq. (12), we find the fiber is dextrorotatory if $\alpha < 0$ and levorotatory in the opposite case. In summary, following these conventions, the previous relations become

$$\epsilon = \frac{2}{L}\,(k\pi \pm \arctan m), \tag{31}$$

$$\alpha = \pm\frac{\epsilon}{m}\tan 2\phi, \tag{32}$$

$$\beta = (\epsilon^2 - \alpha^2)^{1/2}. \tag{33}$$

We see that the measurement of ϕ and ψ cannot completely characterize the matrix of the fiber. Some undetermination remains in the sign of α (is the fiber dextrorotatory or levorotatory?) and in the value of k. In Section 4, we will answer these two questions, and the matrix of the fiber will then be completely defined.

4. Experimental Results

The experimental setup that we used to determine the LSP and the ESP and then to measure the azimuths ϕ and ψ is shown in Fig. 4(a). We will use different linearly polarized laser sources. Before being injected into the fiber during a test, the light passes through either a single wave plate or an association of two wave plates. The first half-wave plate, oriented along θ_1, acts like an azimuth controller (AC), since it rotates only the plane of vibration of an incident linear polarization. The association of the second half-wave plate and the quarter-wave plate, oriented along θ_2 and θ_3, respectively, acts like an ellipticity controller (EC). Indeed, the azimuth of the emerging polarization is fixed by the azimuth θ_3 of one eigenaxis of the quarter-wave plate. We can vary its ellipticity continuously from right-handed to left-handed circular polarization by rotating the half-wave plate. The test fiber is a Nd doped and is used in our laboratory for laser applications. Its exact length is $L = 1.664$ m. The fiber is kept straight in a thin capillary tube for the reason that is outlined in Subsection 4.B. The polarization analyzer allows us to know exactly the output state of polarization. First we present the measurements of the LSP and the ESP.

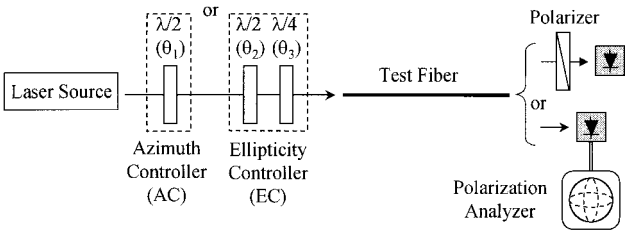

Fig. 4. Experimental setup for the measurement of the LSP and the ESP.

A. Determination of the Linear and Elliptical States of Polarization

In this subsection the laser source is a linearly polarized Nd:YAG laser operating at 1064 nm. The AC and the EC are then formed with wave plates at 1064 nm. To determine the LSP of the fiber, we find the orientation ϕ_{in} of the linear input polarization (by rotating the AC) corresponding to a linear output polarization of azimuth ϕ_{out}. In its own basis, our polarization analyzer gives an output azimuth of $\phi_{out} = -15.6°$ for an injected linear polarization oriented along $\phi_{in} = 41.4°$ (or $\phi_{out} = 74.4°$ and $\phi_{in} = 131.4°$, which are both orientations that are perpendicular to the two previous ones). We conclude that the well-adapted basis ($\mathbf{X}$, $\mathbf{Y}$), in which the Jones matrix of the fiber is written, makes an angle $\phi_0 = (\phi_{in} + \phi_{out})/2 = 12.9°$ with respect to the basis of our polarization analyzer. The respective roles of $\mathbf{X}$ and $\mathbf{Y}$ will be examined later in this paper. The other information obtained from this measurement is the value $2\phi = \phi_{out} - \phi_{in} = -57°$.

Knowing the azimuth ϕ_0 of one eigenpolarization of the fiber, we inject an elliptical polarization of azimuth ϕ_0 and vary its ellipticity (with the EC) until the output polarization is linear. We find an output azimuth of $\psi = -47.5°$ [$\psi = -60.4°$ in the basis ($\mathbf{X}$, $\mathbf{Y}$)] for an input ellipticity of $\xi = -17.7°$. The value of ξ is not needed in our model for us to determine the parameters of the fiber, but it will be compared later with its theoretical value to validate the method. Another way to compare experimental values with theoretical modeling, and then to prove the validity of our experimental method, is to measure the ellipticity of one of the eigenpolarizations of the fiber. This method consists of varying the ellipticity of the input polarization of azimuth ϕ_0 until the output azimuth

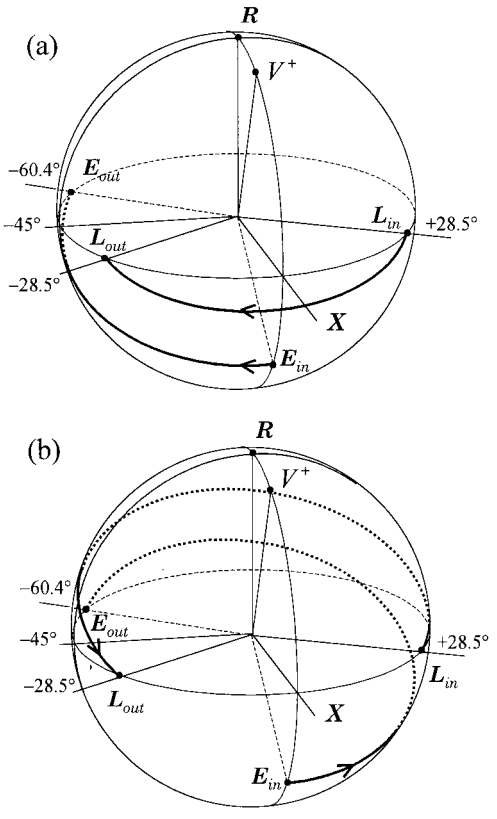

Fig. 5. Possible paths describing the evolution of an input LSP and ESP of the fiber for (a) $\epsilon = 1.24$ rad/m and (b) $\epsilon = 2.53$ rad/m. Note that the angles mentioned on the figure are real values of the azimuth.

also becomes ϕ_0. We find the input and output ellipticities have approximately the same value, equal to $\chi_0 = 33°$. In other words, these input and output states are the same, confirming that it is one eigenpolarization of the fiber. Note that this last measurement provides an important detail: According to Eq. (14) it gives a simple relation between α and ϵ. In our demonstration we compared just this measurement with its theoretical value. However, according to our convention (see Subsection 3C), the knowledge of the sign of χ_0 (positive in our case) is used to call **X** the direction of azimuth ϕ_0 and **Y** the orthogonal direction. We stipulate that the previous measurements are fairly stable and can be reproduced over several days with a drift of less than 1°.

Knowing the basis (**X**, **Y**) and the angles ϕ and ψ we can now determine possible values for the parameters α, β, and ϵ. Indeed, at this stage of our study we cannot know how many times 2π is ϵ (value of k) or the sign of α, so an infinite number of parameters can be calculated. The lower value for ϵ corresponds to $k = 0$ and the + sign in Eq. (31), i.e., $\epsilon = 1.24$ rad/m, corresponding to $\alpha = -1.14$ rad/m and $\beta = 0.50$ rad/m. The second value for the total phase shift ($k = 1$ and the − sign) is $\epsilon = 2.53$ rad/m, corresponding to $\alpha = 2.32$ rad/m and $\beta = 1.02$ rad/m. These two cases are illustrated in Fig. 5, showing the two possible directions of rotation of an input polarization propagating in the fiber. In Fig. 5(a), the input states $\mathbf{L}_{in}$ and $\mathbf{E}_{in}$ become $\mathbf{L}_{out}$ and $\mathbf{E}_{out}$ by clockwise rotation, on the Poincaré sphere, of angle $\epsilon L = 2.06$ rad around the axis defined by the eigenpolarizations of the fiber. In Fig. 5(b), the same input states rotate counterclockwise on an angle $\epsilon L = 4.21$ rad to become the same output linear polarizations. Higher values of ϵ would not change the LSP or the ESP but would change only the number of turns around the rotation axis. Using the two previous sets of values for the parameters, for $\mathbf{V}^+$ our theoretical model predicts an ellipticity χ of 33.1° [according to Eq. (14)] and, for $\mathbf{E}_{in}$, an ellipticity ξ of −17.9° [according to Eq. (22)]. These values are in perfect agreement with our measurements, confirming the good accuracy of our experimental method.

At this stage we have shown that our experimental method allows us to determine the Jones matrix of a given fiber. The method is simple and accurate, since it consists only of measuring the azimuths of three linear polarizations. The parameters extracted from the experiment have physical meaning, since α is the amount of circular birefringence of the fiber, β is the amount of linear birefringence, and (**X**, **Y**) coincides with the azimuth of the eigenpolarizations of the fiber. The Jones matrix is not unique, but each of the possible matrices predicts the same output polarization for a given input polarization. At this stage, we can simulate the evolution of an input linear state at 1064 nm, as will be shown in Subsection 4D.

However, in some cases (in particular in fiber laser studies[6–9]), one has to use a more realistic model that gives the exact value for integer k. Actually, for a fiber length $L = 1.664$ m, ϵ is effectively several times 2π. A magneto-optic method used to evaluate the integer k is presented in Subsection 4.B.

B. Magneto-Optic Method

The effect of an axial magnetic field applied to single-mode optical fibers was first demonstrated by Smith.[21] Some applications have been developed in the domain of isolators, filters, or sensors,[22] and for the measurement of beat lengths of optical fibers.[23–25] Here we propose to use this effect to measure the beat length of our fiber.

The setup of the experiment is shown in Fig. 6(a). The laser source is the previous linearly polarized Nd:YAG laser operating at 1064 nm. The half-wave plate acts as an AC to set the input azimuth to ϕ_{in} (previously measured). The coil, which is 1 cm long and contains 1000 turns, can be translated along the longitudinal direction of the fiber, delivering a local axial magnetic field of approximately 14×10^3 A/m. The fiber is kept in the same configuration as previously shown (straight in a thin capillary tube) to get rid of any mechanical perturbations when the coil is moving. The reason that we use a modulated current and a lock-in amplifier will be discussed later in this paper. The output intensity is detected through an appropriately oriented polarizer. The signal observed on an oscilloscope is periodic while the coil is

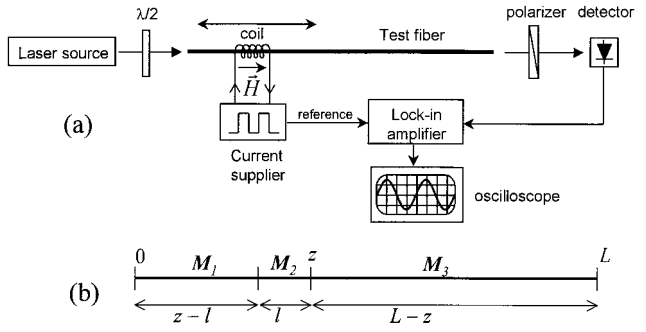

Fig. 6. Setup of (a) the magneto-optic method and (b) modeling of the fiber.

translated along the fiber length. The period is the beat length L_B of the fiber. This length is the one for which the phase shift of the fiber is exactly 2π and then must verify $\epsilon L_B = 2\pi$. In theory, knowledge of L_B should allow us to calculate ϵ.

To understand the principle of this method and the reason we cannot observe the output signal directly, we now propose a brief modeling of the experiment. Note that this modeling considers that the elliptical birefringence of the fiber is constant over the fiber length. This is not strictly correct for low-birefringence fibers submitted to random perturbations but is quite realistic for high-birefringence fibers for which we can expect low birefringence fluctuations over the measurement length. As we will see from the experimental results, our fiber behaves like the latter case and justifies the following mathematical approach.

The fiber can be divided into three sections, each described by an appropriate Jones matrix, as shown in Fig. 6(b). If we call z the longitudinal coordinate of the coil, the first matrix $\mathbf{M}_1$ is the Jones matrix $\mathbf{M}_f$ of the fiber, given by Eqs. (10)–(13) for a fiber of length $z - l$, with l being the length of the coil:

$$\mathbf{M}_1 = \begin{pmatrix} a_1 & b_1 \\ -b_1 & a_1^* \end{pmatrix}, \tag{34}$$

with

$$a_1 = \cos\frac{\epsilon(z-l)}{2} + i\,\frac{\beta}{\epsilon}\sin\frac{\epsilon(z-l)}{2}, \tag{35}$$

$$b_1 = -\frac{\alpha}{\epsilon}\sin\frac{\epsilon(z-l)}{2}. \tag{36}$$

In the section of the fiber subjected to the magnetic field, the Jones matrix of the fiber must be modified to take into account the Faraday effect created by the axial magnetic field. This Faraday effect is a circular birefringence that must be added to the natural birefringence of the fiber. The magnitude of this additional circular birefringence is given by[26]

$$h = 2VH, \tag{37}$$

where V is the Verdet constant that is usually equal to 1.6×10^{-6} rad/A at 1060 nm for fused silica[26] and H is the magnitude of the magnetic field. The magnitude of h can then be evaluated, and we find $h = 0.045$ rad/m. The circular birefringence and the total phase shift in the section of fiber subjected to the magnetic field become

$$\alpha_h = \alpha + h, \tag{38}$$

$$\epsilon_h = (\beta^2 + \alpha_h^2)^{1/2}, \tag{39}$$

and the corresponding matrix $\mathbf{M}_2$ is then

$$\mathbf{M}_2 = \begin{pmatrix} a_2 & b_2 \\ -b_2 & a_2^* \end{pmatrix}, \tag{40}$$

with

$$a_2 = \cos\frac{\epsilon_h l}{2} + i\,\frac{\beta}{\epsilon_h}\sin\frac{\epsilon_h l}{2}, \tag{41}$$

$$b_2 = -\frac{\alpha_h}{\epsilon_h}\sin\frac{\epsilon_h l}{2}. \tag{42}$$

In the final section, $\mathbf{M}_3$ is the Jones matrix $\mathbf{M}_f$ of the fiber whose length is $L - z$:

$$\mathbf{M}_3 = \begin{pmatrix} a_3 & b_3 \\ -b_3 & a_3^* \end{pmatrix}, \tag{43}$$

with

$$a_3 = \cos\frac{\epsilon(L-z)}{2} + i\,\frac{\beta}{\epsilon}\sin\frac{\epsilon(L-z)}{2}, \tag{44}$$

$$b_3 = -\frac{\alpha}{\epsilon}\sin\frac{\epsilon(L-z)}{2}. \tag{45}$$

To perform the derivation of the matrix $\mathbf{M}_h = \mathbf{M}_3\mathbf{M}_2\mathbf{M}_1$ of the whole fiber, we must take into account that $l \ll L$ and $h \ll \alpha$. Then, making limit developments and keeping only the first-order terms in l or h, we find, after some lengthy and cumbersome algebra,

$$\mathbf{M}_h = \begin{pmatrix} A_h & B_h \\ -B_h^* & A_h^* \end{pmatrix}, \tag{46}$$

with

$$A_h = \cos\frac{\epsilon L}{2} + i\,\frac{\beta}{\epsilon}\sin\frac{\epsilon L}{2} - ih\,\frac{\alpha\beta}{\epsilon^3}\left(1 - h\,\frac{\alpha}{\epsilon^2}\right) \times \sin\frac{\epsilon_h l}{2}\cos\frac{\epsilon(L + l - 2z)}{2}, \tag{47}$$

$$B_h = -\frac{\alpha}{\epsilon}\sin\frac{\epsilon L}{2} - h\,\frac{\beta^2}{\epsilon^3}\sin\frac{\epsilon_h l}{2}\cos\frac{\epsilon(L + l - 2z)}{2} - ih\,\frac{\beta}{\epsilon^2}\left(1 - h\,\frac{\alpha}{\epsilon^2}\right)\sin\frac{\epsilon_h l}{2}\sin\frac{\epsilon(L + l - 2z)}{2}. \tag{48}$$

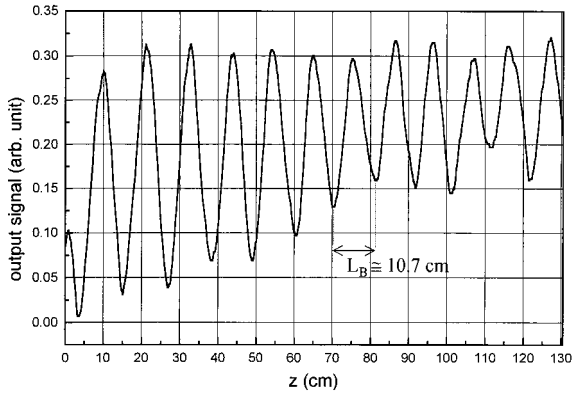

Fig. 7. Measurement of the beat length of the fiber at 1064 nm with the magneto-optic method.

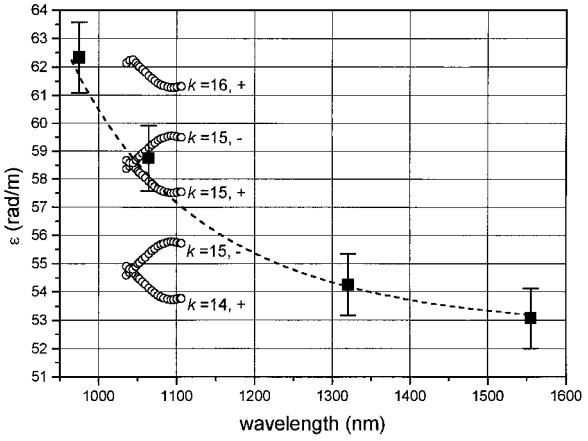

Fig. 8. Measurement of ϵ as a function of wavelength by use of the magneto-optic method (squares) and the LSP–ESP method (circles).

Finally, to calculate the intensity of light detected after the polarizer, we must derive the intensity of the output Jones vector defined by

$$\mathbf{V}_{\text{out}} = \mathbf{M}_p(\phi + \pi/4)\mathbf{M}_h\mathbf{E}_{\text{in}}, \tag{49}$$

where $\mathbf{E}_{\text{in}}$ is the Jones vector of an input LSP of the fiber in the absence of the magnetic field (linear polarization oriented along $-\phi$) and $\mathbf{M}_p(\phi + \pi/4)$ is the Jones matrix of a polarizer oriented at 45° with respect to the azimuth of the corresponding output LSP in the absence of the magnetic field (linear polarization oriented along ϕ). Note that ϕ is given by Eq. (18). The choice of 45° in the previous relation simplifies the calculation of $\mathbf{V}_{\text{out}}$. However, some lengthy algebra and the same approximations as those used previously are necessary to find a simple formula for the intensity I_{out} of the normalized vector $\mathbf{V}_{\text{out}}$:

$$I_{\text{out}} = \frac{1}{2} + h\,\frac{\beta^2}{\epsilon^3}\sin\frac{\epsilon_h l}{2}\cos\frac{\epsilon(2L + l - 2z)}{2}. \tag{50}$$

This expression confirms that I_{out} is periodic as a function of z and that the period is $2\pi/\epsilon$, which is the beat length L_B of the fiber in the absence of the magnetic field. The constant $1/2$ in Eq. (50) is the output intensity when no current supplies the coil ($h = 0$). The reason for this is that we detect the signal through a polarizer oriented at 45° with respect to the output LSP. Applying a cw current to the coil leads to an oscillation of the output polarization around the output LSP and then modulates the output intensity when the coil is moving. We evaluated the magnitude of this modulation. At maximum it is equal to h/ϵ. According to both the value of h (calculated previously) and the value of ϵ (we expect to be several times 2π), h/ε is of the order of 10^{-3} and then much lower than $1/2$. For this reason we modulate the current supplier at a frequency of approximately 5 kHz and detect the signal through a lock-in amplifier. This method allows us to extract the modulated part of I_{out}.

Figure 7 shows the experimental result. Our experimental apparatus limits the displacement of the coil to 130.5 cm. The decrease of the amplitude of the modulation may traduce the inhomogeneity of the fiber or may be due to our experimental apparatus. However, we note that the elliptical birefringence of this fiber remains approximately constant, proving that in our case the assumption of random fluctuations of birefringence fails. The behavior of our fiber is close to that of polarization-maintaining fibers[25] and validates our theoretical modeling of the magneto-optic method. A good evaluation of the beat length of the fiber is obtained, and we find $L_B = 10.7 \pm 0.2$ cm. The evaluation of the quantity ϵL then yields $(15.56 \pm 0.3)2\pi$ rad for $L = 166.4$ cm. According to Eq. (31), the accuracy of this value is not high enough to determine with precision the integer k (which can be 15 or 16) and the sign of α. The next step, which will permit us to have the exact value of our parameters, is to take measurements as a function of the wavelength.

C. Wavelength Dependence

Two experiments are presented in this section. We first measure the beat length of the fiber (using the MO method) with various laser sources. In addition to the previous source operating at 1064 nm, we realize the measurements at 975, 1320, and 1555 nm. The results are shown in Fig. 8 (black squares), where error bars of $\pm 2\%$ take into account the accuracy of the method. This curve indicates that ϵ decreases versus the wavelength, which is a well-known result. The dashed curve just acts as a guideline for the eyes.

The second experiment measures the three particular angles ϕ_{in}, ϕ_{out}, and ψ for various wavelengths in the range 1036–1104 nm and then calculates the parameters α, β, and ϵ. This can be realized with the help of a tunable Yb-doped double-clad fiber laser that is available in our laboratory.[27] First, we present in Fig. 9 the experimental values of these angles measured with a step of approximately 4 nm. In this figure the angles are the real values measured

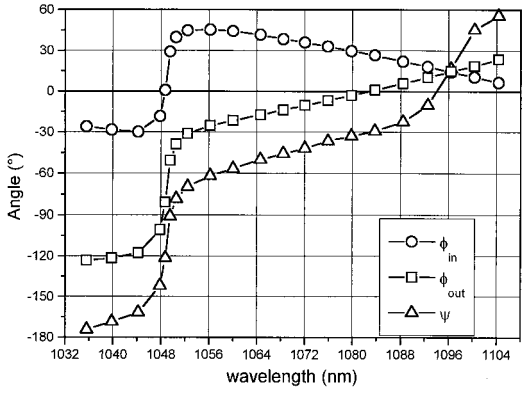

Fig. 9. Experimental measurement of ϕ_{in}, ϕ_{out}, and ψ as a function of wavelength.

by the polarization analyzer in its own basis. For each wavelength we can now calculate α, β, and ϵ according to Eqs. (31)–(33). Several sets of parameters can be found, depending on the value of k and the + or − sign that we use in the formulas. This is the reason that possible values of ϵ (open circles) calculated with the value of k and the signs indicated in the figure are also represented in Fig. 8. We clearly see that for $k = 15$ and the + sign the curve is close to the previous measurements that were obtained with the magneto-optic method.

These two experiments then permitted us to determine the exact value of k and the sign to use in the model for the fiber. According to Eqs. (31)–(33), we are now able to confirm definitely that at 1064 nm our 1.664-m-long fiber acts like an elliptical birefringent with the following parameters: $\epsilon = 57.92$ rad/m, $\alpha = -53.73$ rad/m, and $\beta = 21.57$ rad/m. At this wavelength, the fiber is therefore dextrorotatory.

This last experiment also allows us to study the evolution of the parameters, especially α and β versus the wavelength of the injected signal. This is shown in Fig. 10. Although ϵ decreases slightly from 58.7 to 57.5 rad/m, we observed that α and β vary significantly. The value of β always remains positive (because of our convention), whereas α can be either positive or negative. Let us examine in more detail

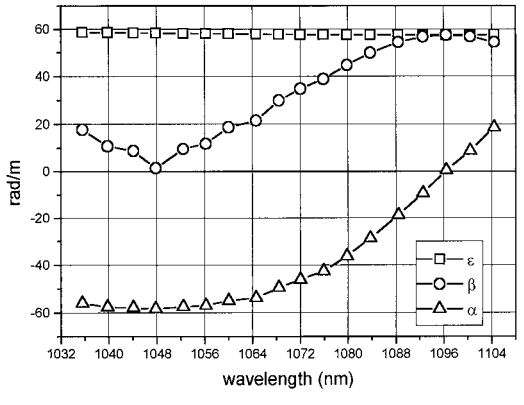

Fig. 10. Wavelength dependence of α, β, and ϵ.

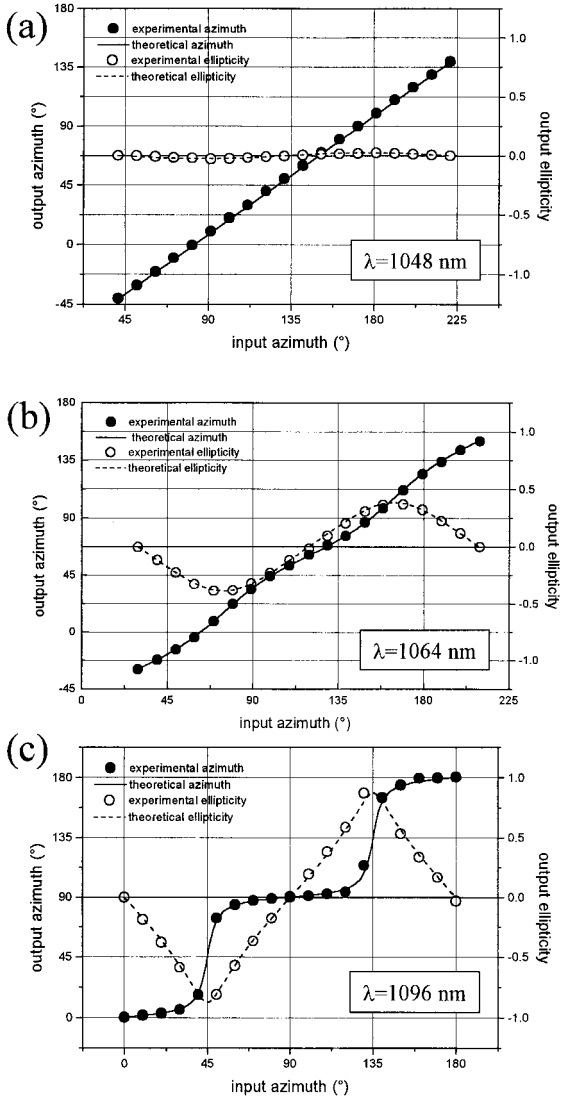

Fig. 11. Evolution of the azimuth and the ellipticity of the output state of polarization versus the input azimuth at (a) 1048, (b) 1064, and (c) 1096 nm.

two wavelengths in particular: at 1048 nm $\beta \approx 0$, and the Jones matrix of the fiber acts almost like a purely circular birefringent plate, with $\alpha = -58.35$ rad/m; at 1096 nm $\alpha \approx 0$, and the fiber acts almost like a purely linear retarder, with $\beta = 57.5$ rad/m. To confirm these new results let us examine the transformation by the fiber of an input linear state as a function of its orientation.

D. Evolution of an Input Linear State

In this experiment we vary the azimuth of an input linear polarization (by a step of 10°) and measure the output state of polarization. This experiment is repeated for three wavelengths: 1048, 1064, and 1096 nm. The evolution of the azimuth and the ellipticity of the measured output state of polarization versus the input azimuth are represented in Fig. 11 for each wavelength. The theoretical prediction of our model is also presented for comparison. Table 1 summa-

Table 1. Parameters Used in the Model

λ (nm)	1048	1064	1096
α^a	−58.35	−52.93	0.57
β^a	1.52	23.43	57.50
ϵ^a	58.37	57.88	57.51

[a]rad/m

rizes the values of the parameters, extracted from experiments, that we used in our model to simulate the evolution of the azimuth and the ellipticity in Fig. 11. First, we note the good agreement between theory and experiment, proof that our method of extraction of fiber parameters is reliable. Second, Fig. 11(a) confirms that at 1048 nm the fiber acts approximately like a circular birefringent plate, conserving the ellipticity of the input polarization and rotating its azimuth on an angle equal to -1.42 rad modulo π (or $-82°$ mod. 180°), which corresponds to the value of $\epsilon L/2$ at this wavelength. According to Fig. 11(c), we note that the behavior of the fiber is close to one of a particular linear birefringent plate: a quarter-wave plate. Indeed, at 1096 nm, the phase difference of $\epsilon L = 57.51$ rad is close to $\pi/2 + 15 \times 2\pi$. At this stage, further investigation is needed to establish the theoretical modeling of the wavelength dependence of parameters α, β, and ϵ.

5. Conclusion

We have modeled the polarization properties of an optical doped fiber by a simple Jones matrix. Because of the complicated nature of the birefringence in optical fibers, for the most general case we had to use the Jones matrix of an elliptical birefringent plate. Instead of using three parameters to express this matrix in an arbitrary basis, we have shown that only two parameters (α and β) and knowledge of the basis (**X**, **Y**) in which the matrix is written are sufficient. These two parameters can be related to the circular (α) and linear (β) part of the elliptical birefringence. The basis (**X**, **Y**) has a simple physical meaning. Algebraic manipulations of this model have led us to find particular angles (ϕ and ψ) that allow us to extract a method of measurement of α, β, and (**X**, **Y**) for a given fiber at a particular wavelength. This method has been presented and allows us to find an infinite number of sets of parameters α and β leading to the same Jones matrix. Any of these sets of parameters can be used to predict the output state of polarization when we know the input state. However, in some applications one needs to know the exact value of the total phase shift and the direction of rotation in the fiber. This is why we have presented the magneto-optic method and have made some measurements at different wavelengths. Finally we have proposed a realistic model, taking into account the polarization properties of the fiber. Wavelength dependence studies have shown that, depending on the wavelength, the fiber continuously evolves from a purely circular birefringent plate to a purely linear one. These new results appear to be useful in studying the polarization properties of doped-fiber lasers or amplifiers.

Appendix A: Relations between Jones Vectors, Stokes Parameters, and Ellipticity and Azimuth

In the most general case, the Jones vector representing an elliptical state of polarization has two complex coordinates and can be written as

$$V = \begin{pmatrix} a + ib \\ c + id \end{pmatrix}. \tag{A1}$$

The Stokes parameters of vector V can be written as

$$s_0 = a^2 + b^2 + c^2 + d^2, \tag{A2}$$

$$s_1 = a^2 + b^2 - c^2 - d^2, \tag{A3}$$

$$s_2 = 2(ac + bd), \tag{A4}$$

$$s_3 = 2(ad - bc). \tag{A5}$$

Ellipticity χ and azimuth φ of the state of polarization represented by V can be expressed as follows:

$$\sin 2\chi = \frac{s_3}{s_0}, \tag{A6}$$

$$\tan 2\varphi = \frac{s_2}{s_1}. \tag{A7}$$

The authors thank P. Pellat-Finet and G. Martel and M. Brunel for their comments on the manuscript.

References

1. I. P. Kaminow, "Polarization in optical fibers," IEEE J. Quantum Electron. **QE-17,** 15–22 (1981).
2. S. C. Rashleigh, "Origins and control of polarization effects in single-mode fibers," IEEE J. Lightwave Technol. **LT-1,** 312–331 (1983).
3. D. Andresciani, F. Curti, F. Matera, and B. Daino, "Measurement of the group-delay difference between the principal states of polarization on a low birefringence terrestrial fiber cable," Opt. Lett. **12,** 844–846 (1987).
4. C. D. Poole, N. S. Bergano, R. E. Wagner, and H. J. Schulte, "Polarization dispersion and principal states in a 147-km undersea lightwave cable," IEEE J. Lightwave Technol. **6,** 1185–1190 (1988).
5. C. D. Poole and R. E. Wagner, "Phenomenological approach to polarization dispersion in long single-mode fibers," Electron. Lett. **22,** 1029–1030 (1986).
6. T. Chartier, F. Sanchez, G. Stéphan, P. Le Boudec, E. Delevaque, R. Leners, and P. L. François, "Channeled spectrum of a fiber laser," Opt. Lett. **18,** 355–357 (1993).
7. U. Ghera, N. Friedman, and M. Tur, "Polarization related phenomena in Nd-doped fiber lasers," Opt. Mater. **4,** 73–80 (1994).
8. H. Y. Kim, S. K. Kim, H. J. Jeong, H. K. Kim, and B. Y. Kim, "Polarization properties of a twisted fiber laser," Opt. Lett. **20,** 386–388 (1995).
9. H. Y. Kim, E. H. Lee, and B. Y. Kim, "Polarization properties of fiber lasers with twist-induced circular birefringence," Appl. Opt. **36,** 6764–6769 (1997).
10. R. Ulrich and A. Simon, "Polarization optics of twisted single-mode fibers," Appl. Opt. **18,** 2241–2251 (1979).
11. E. M. Frins and W. Dultz, "Rotation of the polarization plane

in optical fibers," IEEE J. Lightwave Technol. **LT-14,** 144–147 (1996).
12. G. D. Van Wiggeren and R. Roy, "Transmission of linearly polarized light through a single-mode fiber with random fluctuations of birefringence," Appl. Opt. **38,** 3888–3892 (1999).
13. C. D. Poole and D. L. Favin, "Polarization-mode dispersion measurements based on transmission spectra through a polarizer," IEEE J. Lightwave Technol. **12,** 917–929 (1994).
14. M. Monerie and L. Jeunhomme, "Polarization mode coupling in long single-mode fibres," Opt. Quantum Electron. **12,** 449–461 (1980).
15. C. D. Poole, "Measurement of polarization-mode dispersion in single-mode fibers with random mode coupling," Opt. Lett. **14,** 523–525 (1989).
16. R. C. Jones, "A new calculus for the treatment of optical systems. I. Description and discussion of the calculus," J. Opt. Soc. Am. **31,** 488–493 (1941).
17. R. C. Jones, "A new calculus for the treatment of optical systems. VII. Properties of the **N**-matrices," J. Opt. Soc. Am. **38,** 671–685 (1948).
18. S. Betti, F. Curti, B. Diano, G. De Marchis, E. Iannone, and F. Matera, "Evolution of the bandwidth of the principal states of polarization in single-mode fibers," Opt. Lett. **16,** 467–469 (1991).
19. F. Maystre and R. Dandliker, "Polarimetric fiber optical sensor with high sensitivity using a Fabry–Perot structure," Appl. Opt. **28,** 1995–2000 (1989).
20. E. Hecht and A. Zajac, *Optics*, (Addison-Wesley, Reading, Mass., 1974).
21. A. M. Smith, "Polarization and magnetooptic properties of single-mode optical fiber," Appl. Opt. **17,** 52–56 (1978).
22. G. W. Day, D. N. Payne, A. J. Barlow, and J. J. Ramskov-Hansen, "Faraday rotation in coiled, monomode optical fibers: isolators, filters, and magnetic sensors," Opt. Lett. **7,** 238–240 (1982).
23. M. Turpin, M. Valentin, J. Dubos, and J. Auge, "Mesure de la biréfringence des fibres optiques monomodes à maintien de polarisation linéaire," Rev. Tech. Thomson-CSF **15,** 1049–1071 (1983).
24. P. G. Zhang and D. Irvine-Halliday, "Measurement of the beat length in high-birefringent optical fiber by way of magneto-optic modulation," J. Lightwave Technol. **12,** 597–602 (1994).
25. D. Irvine-Halliday, M. R. Khan, and P. G. Zhang, "Beat-length measurement of high-birefringence polarization-maintaining optical fiber using the DC Faraday magneto-optic effect," Opt. Eng. **39,** 1310–1315 (2000).
26. H. Y. Kim, B. K. Kim, S. H. Yun, and B. Y. Kim, "Response of fiber lasers to an axial magnetic field," Opt. Lett. **20,** 1713–1715 (1995).
27. A. Hideur, T. Chartier, and F. Sanchez, "Yb-doped double-clad fiber laser in a unidirectional ring cavity," in *Optical Devices for Fiber Communication II*, M. J. Digonnet, O. S. Gebizlioglu, R. A. Greenwell, D. N. Horwitz, and D. K. Paul, eds., Proc. SPIE **4216,** 15–21 (2001).